Available online at www.sciencedirect.com
ScienceDirect
Genomics 88 (2006) 779–790
GENOMICS
www.elsevier.com/locate/ygeno

Fourteen novel human members of mitochondrial solute carrier family 25 (SLC25) widely expressed in the central nervous system

Tatjana Haitina, Jonas Lindblom, Thomas Renström, Robert Fredriksson *

Unit of Pharmacology, Department of Neuroscience, Uppsala University, BMC, Uppsala SE 75124, Sweden

Received 5 May 2006; accepted 28 June 2006
Available online 1 September 2006

Abstract

Members of the solute carrier family 25 (SLC25) are known to transport molecules over the mitochondrial membrane. In this paper we present 14 novel members of SLC25 family in human. These were provided with following gene symbols by the HGNC: SLC25A32, SLC25A33, SLC25A34, SLC25A35, SLC25A37, SLC25A38, SLC25A39, SLC25A40, SLC25A41, SLC25A42, SLC25A43, SLC25A44, SLC25A45, and SLC25A46. We also identified the orthologues for these genes in rat and mouse. Moreover, we found yeast orthologues for 9 of these genes and show that the predicted substrate binding residues are highly conserved in the human and yeast proteins. We performed a comprehensive tissue localization study for 9 of these genes on a panel of 30 rat tissues with quantitative real-time polymerse chain reaction. We detected their mRNA in a wide number of tissues, both in brain and in periphery. This study provides an overall roadmap of the repertoire of the SLC25 family in mammals, showing that there are at least 46 genes in the human genome coding for mitochondrial transporters.

Keywords: Mitochondrial transporter; SLC; Human; Rat; Mouse; Expression

Genes coding for membrane proteins comprise one of the largest groups of genes in the vertebrate genome. Genes for membrane proteins are claimed to constitute more than 10% of all genes in the human [1] and mouse [2] genomes. Important subgroups of membrane proteins are G-protein-coupled receptors [3], single-pass tyrosine kinase receptors [4], ion channels [5], and solute carriers [6]. Solute carriers control the uptake and flow of various substances such as sugar, amino acids, nucleotides, inorganic ions, and drugs over the cell membrane and there are currently 43 known families of solute carriers [6].

The solute carrier family 25 (SLC25) consists of proteins that function as transporters of a large variety of molecules. This is a family of structurally and functionally related proteins that contain six α-helical membrane-spanning regions [7]. All of the characterized SLC25s, with the exception of SLC25A17, which is located in peroxisomal membrane [8], are localized to the inner mitochondrial membrane [9] and are hence referred to as mitochondrial carriers. In the most recent overview [9] 23 functionally known members of the SLC25 family were presented, SLC25A1–SLC25A22 and SLC25A27. Since then, an additional 9 proteins have been annotated from the various human genome annotation projects and presented in the Ensembl gene lists (http://www.ensembl.org).

The molecules transported by the SLC25 family of proteins include ATP/ADP, amino acids (glutamate, aspartate, lysine, histidine, and arginine), malate, ornithine, and citruline [9]. All these molecules originate from macromolecules that constitute the energy sources of cells and which are broken down into less complex molecules by cellular enzymes. These metabolic intermediates are transported into the mitochondria to be converted into energy via oxidation, energy that is used to maintain the proton gradient over the inner mitochondrial membrane. That potential energy stored in this gradient is utilized to drive the phosphorylation of ADP to produce ATP, the main form of energy in the cell.

SLC25A7, SLC25A8, and SLC25A9, also known as uncoupling proteins (UCP) 1, 2, and 3, have been shown to transport protons directly [10] and these are among the most well-studied members of the SLC25 family. They are referred to

* Corresponding author. Fax: +46 18 51 15 40.
E-mail address: robert.fredriksson@bmc.uu.se (R. Fredriksson).

0888-7543/$ - see front matter © 2006 Elsevier Inc. All rights reserved.
doi:10.1016/j.ygeno.2006.06.016

as uncoupling proteins because they are responsible for decoupling the electron transportation chains that exist across the inner mitochondrial membrane and thereby enable energy to be released as heat instead of being converted into ATP. In addition to these "classical" UCP proteins, two others, SLC25A27 (UCP4) and SLC25A14 (UCP5 or BMCP1), have been discovered and these have been shown to mediate mitochondrial uncoupling [11,12]. Several of the UCPs are expressed in the central nervous system (CNS); for example, *SLC25A8* (UCP2) is highly expressed in the hypothalamus, pituitary, and brainstem [13] but is also widely expressed in the periphery [14]. *SLC25A27* (UCP4) and *SLC25A14* (UCP5 or BMCP1) are, on the other hand, relatively selectively expressed in the CNS [15]. BMCP1 has by in situ hybridization in mice been shown to be highly expressed in hypothalamus, hippocampus, thalamus, and amygdala [12,16] while UCP4 is broadly expressed in the brain [11]. These proteins have been shown to be important in healthy neurons for energy production and to have a role in neuronal signaling [17]. Mitochondrial UCPs have also been suggested to have a role in neurodegenerative diseases such as Parkinson's disease, Alzheimer's disease and ALS and in normal aging of the brain [15]. Although the UCPs have been relatively extensively studied in the CNS, the role of other SLC25 members in brain is fairly unknown.

In this study we identified 14 novel genes that belong to the SLC25 family. We performed phylogenetic analyses of these genes in humans and rodents and discuss their relationship to the previously known members of the family. We also performed an extensive tissue localization study for 9 of these novel genes in rat with the quantitative real-time PCR (qPCR) technique and show that their mRNA is found in a wide number of tissues, including several distinct brain regions. This study shows that the SLC25 family has at least 46 members in humans, making it by far the largest of the 43 SLC families.

Results

A dataset consisting of 29 SLC25 sequences, SLC25A1–SLC25A29, was obtained by downloading all SLC25 sequences present in the SLC database at http://www.bioparadigms.org/slc/menu.asp. This dataset was considered the seeding set and from these sequences a sequence HMM model was constructed. Four different databases, RefSeq, Ensembl peptides, Ensembl AbInitio, and the human subset of the Mammalian Gene Collection (MGC), were all searched against that model and all hits were extracted. After filtration by BLAST searches against the human RefSeq database, removal of possible pseudogenes, and manual curation, 17 sequences not present in the seeding set remained. Three of these were found as annotated sequences in the UCSC known gene track in the UCSC genome database at http://genome.ucsc.edu/ as *SLC25A30*, *SLC25A31*, and *SLC25A36*. The other 14 sequences were considered novel and through communication with the HUGO gene nomenclature committee the novelty of these sequences was confirmed and new gene symbols were allocated. Below we present the origin and database status of each of these 14 sequences.

SLC25A32: This sequence was represented in GenBank by four identical human mRNA sequences, BC021893, AK027787, AF283645, and AK027531, which contain the complete coding region. It was also represented by another mRNA sequence, AK027531, which contains an alternative intron in the last exon. The sequence was found to be supported by over 100 EST sequences.

SLC25A33: The *SLC25A33* sequence had seven (CR594441, CR620898, CR593565, BC073135, AJ880283, BC004991, and AF495714) full-length mRNAs supporting its entire coding region. There was also one other sequence, CR595626, which contained one extra, in-frame, exon between exons 2 and 3, representing a possible splice variant. In addition this sequence was found to be present as an MGC clone (number 4399) and was supported by over 100 EST sequences.

SLC25A34: This sequence had one mRNA sequence, BC027998, supporting its entire coding region and two partial mRNA sequences, CR749264 and AL832282, supporting its most C-terminal exon. In addition there were 11 ESTs supporting this sequence.

SLC25A35: The *SLC25A35* sequence had its entire coding region supported by four mRNA sequences, AK097536, BC041597, BC052233, and BC101329. In addition we found two identical full-length mRNA sequences, BC101330 and AY498866, with one additional in-frame exon between exons 4 and 5, which very likely represent functional splice variants of the *SLC25A35* sequence.

SLC25A37: The sequence version of *SLC25A37* that we used for our analysis was found to be supported by one mRNA sequence, which covers the entire coding region of *SLC25A37*. In addition there are seven mRNAs (AK074708, AK223194, AY032628, CR592142, BC015013, AK075313, and AL833186) with alternative 5' splice junctions for the second exon resulting in a longer exon. None of these seems to be functional as elongation of the second exon resulted in an interrupted open reading frame. This, together with the fact that all seven sequences had different 5' splice junctions suggests a weak splice signal. The *SLC25A37* sequence was also supported by over 100 EST sequences and over 20% of these ESTs supported the functional splice variant that we used for our analysis.

SLC25A38: This sequence had six identical mRNA sequences (AK000558, CR614324, CR619847, CR591050, BC013194, and CR457242) supporting its entire coding region and two partial mRNA sequences (CR621188 and AK026356) supporting its two most C-terminal exons. In addition there were over 100 ESTs supporting this sequence.

SLC25A39: In total, this sequence was supported by 37 mRNAs that cover the entire coding region. The *SLC25A39* sequence appeared to be present in two splice variants with an alternative 3' splice junction at the fourth exon resulting in an eight-amino-acid-longer exon. Representative mRNAs for the shorter variant are AF151827, AB209576, BC009330, CR601587, and CR597204 while the longer variant was supported by, for example, BC096819, CR605651, CR594793, CR610093, and CR605364. In total, the short and long variants

were supported by 26 and 11 mRNAs, respectively. In addition to the mRNA sequences, the *SLC25A39* was supported by over 100 ESTs.

SLC25A40: The *SLC25A40* was included in the RefSeq database as mitochondrial carrier functional protein (MCFP) and its entire coding region is supported by five full-length mRNAs (CR610506, BC027322, AK223020, AF125531, and CR609204). In addition to the mRNA sequences, this sequence was supported by 98 ESTs.

SLC25A41: This protein was supported by two mRNA sequences, BC031671 and AK097761, and the latter of these represents a functional splice variant with one extra in-frame exon between exons 2 and 3. *SLC25A41* is also present in the MGC cDNA database as MGC34725. It is notable that all sequences representing the human SLC25A41 are missing five amino acids, including the first methionine in the first exon, compared to orthologue sequences in rodents. There can be two possible explanations for this: either there could be another functional start codon further downstream in exon 1 or there is one additional exon upstream that contains the start of the coding sequence. We consider the second alternative to be the most likely as the amino acid sequence in exon 1, except the five missing amino acids, is well conserved and because no likely ribosomal entry sequence could be found in exon 1. Therefore, the sequence presented in this paper is partial. The sequence of *SLC25A41* was supported by seven ESTs.

SLC25A42: The *SLC25A42* was present in the MGC as MGC26694, which contains the entire coding sequence. Apart from that, the sequence was supported by one full-length mRNA (BC045598), which contains one extra in-frame exon between exons 2 and 3. This is likely to represent a functional splice variant. The sequence is also supported as being truly expressed by 64 ESTs.

SLC25A43: The sequence for *SLC25A43* is supported by five mRNAs that cover the entire coding sequence. Two of these (BC019584 and BC071871) are identical to the sequence that we used for our analysis, while two other (AK091304 and AX746905) support a functional splice variant with one extra exons between exons 3 and 4 and the fifth mRNA has one extra intron in exon 1. The sequence is also supported by 35 ESTs.

SLC25A44: This sequence has five mRNA sequences (AK074912, BC008843, AK075002, AB007915, and BC039854) supporting its entire coding region. In addition to the mRNA sequences we found over 100 ESTs supporting this sequence.

SLC25A45: The SLC25A45 protein was supported by six mRNAs, which in total represents four functional splice variants. The version used in this paper is represented by BC041100. Compared to this sequence, one variant with an extra exon between exons 2 and 3 is represented by mRNA sequences BC036869 and CR591170. Another variant with the same extra exon between exons 2 and 3, but also lacking the third exon that is present in BC041100, is represented by AY597807. The fourth variant was supported by two mRNA sequences, AK091190 and AX746837. It is similar to the second variant described, with the exception that it has one extra exon between exons 1 and 2 and the 3' splice junction for exon 2 (i.e., the third exon for this variant) is further upstream in the sequence resulting in a longer exon. The *SLC25A45* sequence was supported by 20 ESTs.

SLC25A46: The *SLC45A46* was present in the RefSeq database as LOC91137. Its coding region is supported by three full-length mRNA sequences (AK091427, BC017169, and M74089) and one partial mRNA (BX648087) that covers the first three exons. The sequence was supported by over 100 ESTs.

We retrieved 14 rat and 14 mouse sequences from genome databases and with a help of alignment and phylogenetic analysis (data not shown) we confirmed that those were the orthologues of our novel human SLC25 family members. All the sequences that we assembled are included in the supplementary material. Amino acid identity analysis is presented in Supplementary Table 1. The percentage identity within this family varies from 92% for the most similar pair of sequences (SLC25A5 and SLC25A6) to 10% for the least similar pair (SLC25A2 and SLC25A46). A phylogenetic tree was constructed with all already known and novel human SLC25 family members together with 10 yeast SLC25 family proteins. This tree is presented in Fig. 1. The novel human sequences were spread through the tree and most of them display paralogous relationships to previously reported SLC25 proteins.

We performed an expression analysis of rat UCP2 and nine of the novel rat SLC25 family members in a range of tissues. Eight coronal sections of rat brain (Fig. 2), hypothalamus, brainstem, hindbrain (cerebellum, pons, and medulla oblongata), pituitary gland, cerebellum, spinal cord, pineal gland, eye, adrenal gland, skeletal muscle, adipose tissue, heart, intestine, kidney, liver, lung, spleen, thymus, ovary, uterus, testis, and epididymis were isolated and used for RNA isolation and cDNA synthesis. Two housekeeping genes histone 3 (H3) and ribosomal protein L19 (RPL19) were used to calculate normalization factors. The gene expression stability measures were 0.662 and 0.646 for H3 and RPL19, respectively. The relative expression values (% ± SD%) for UCP2, *Slc25a32*, *Slc25a37*, and *Slc25a40-46* are presented on Fig. 3 and in Supplementary Table 2. The relative expression of UCP2 was highest in the pituitary gland, kidney, heart, and adrenal gland. We were not able to detect the transcript in the brain coronal sections I and II. The highest levels of *Slc25a33* were detected in the brainstem, coronal section VIII, coronal section IV, and pineal gland. The expression levels of *Slc25a37* were highest in brain sections II and I, testis, and liver. We did not find the *Slc25a37* transcript in hypothalamus, pineal gland, intestine, and epididymis. The highest levels of *Slc25a40* were detected in coronal section I, coronal section II, cerebellum, and coronal section VII. The transcript for *Slc25A41* was detected only in coronal sections I to VII, liver, and testis and at very low level in epididymis. The highest expression was in coronal sections I and II. *Slc25a42* had very high transcript levels in adipose tissue. The next highest levels were detected in brain section VII, hypothalamus, and section IV. *Slc25a43* was detected at

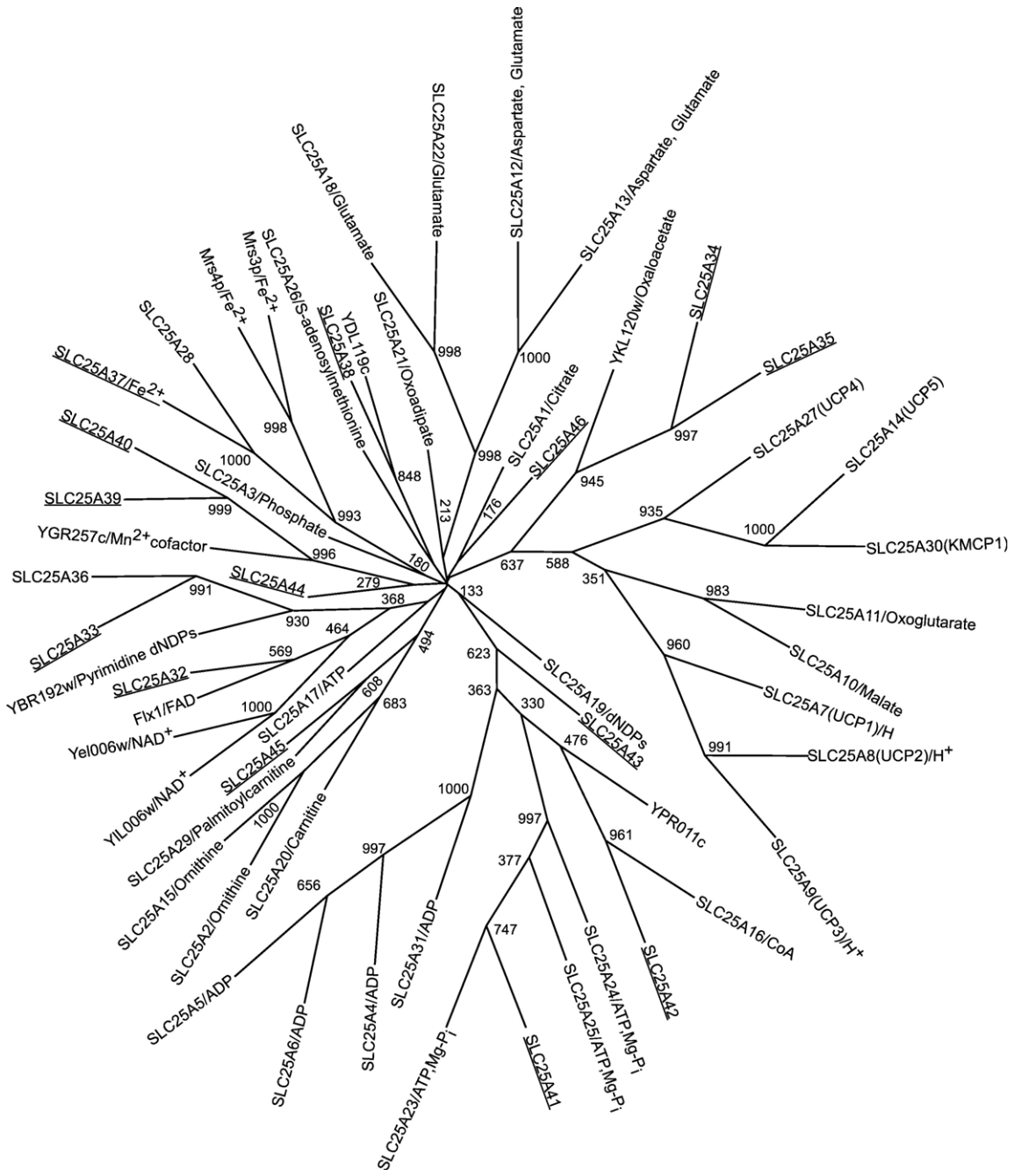

Fig. 1. Phylogenetic analysis of full-length amino acid sequences of human SLC25A1-46 and 10 yeast SLC25 family members. The consensus tree was generated by Neighbor-Joining analysis (Phylip 3.6). The numbers at the nodes indicate bootstrap replicates. The novel sequences are underlined. The preferred substrate, if known, is stated after the slash. The accession numbers are listed under Materials and methods.

highest levels in sections II and I, followed by adrenal gland and skeletal muscle. The relative expression of *Slc25a44* was highest in hindbrain, brain sections IV and VII, and cerebellum. Levels of *Slc25a45* were highest in coronal section I, skeletal muscle, intestine, and coronal section II. The transcripts for neither *Slc25a43* nor *Slc25a45* were detected in hypothalamus. The expression of *Slc25a46* was detected as highest in hindbrain, coronal section IV, spinal cord, and section VII.

In general, the UCP2, *Slc25a42*, and *Slc25a46* had the highest expression levels of all the SLC25 family members tested in this study. Overall, the expression was lowest for *Slc25a37* and *Slc25a40* in all tested tissues.

Discussion

We have identified 14 new human members of the solute carrier family 25 (SLC25). We also identified their orthologues in mouse and rat. The new transporters were approved by the HUGO gene nomenclature committee and were given the gene symbols *SLC25A32–A35* and *SLC25A37–SLC25A46* (Table 1). Taking into consideration the amount of genomic data, ESTs,

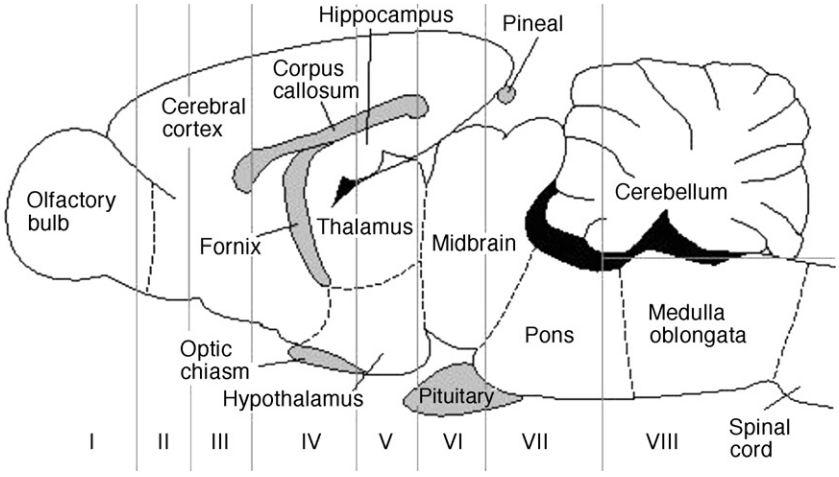

Fig. 2. Schematic presentation of rat brain coronal sections. The sections are marked with Roman numerals.

and mRNA sequences that we analyzed in this study, it is unlikely that there exist additional members of the SLC25 family in humans. We therefore conclude that the repertoire of the SLC25 family is fairly complete with 46 members in humans and 45 members in mice and rats. This makes the SLC25 family the largest of the 43 SLC families.

All the novel solute carriers exhibit the common features characteristic for the SLC25 family, such as complex genomic structure with a large number of exons. They also have a similar secondary structure with six predicted transmembrane helices. We have performed amino acid identity analysis (Supplementary Table 1) and constructed a phylogenetic tree for all known human SLC25 proteins together with 10 yeast proteins from the same family [22] (Fig. 1). The expression of all novel solute carriers is supported by EST data and we present quantitative real-time PCR data for nine of them. Together the results indicate that all of the 14 sequences belong to the SLC25 family and are most likely functional proteins. Our phylogenetic analysis is consistent with previously published trees [9] and shows a clear clustering of carriers transporting the same substrate (Fig. 1). It has been previously shown for solute carrier family 6 (SLC6) that phylogenetically related proteins have the same or similar substrates [28]. Therefore we were encouraged to speculate about the possible substrate preference and functional properties of newly identified SLC25 family members.

SLC25A34 and SLC25A35 display 45% amino acid identity to each other and branched basal of the UCP/DIC/OGC cluster in the phylogenetic tree. The similarity is further supported by local blast search, which simultaneously displays SLC25A11 as the closest relative with 26–33% amino acid identity. SLC25A35, SLC25A11, and SLC25A10 are all located on human chromosome 17 (see Fig. 4), which might indicate a common origin. Interestingly, the phylogenetic analysis revealed that SLC25A34 and SLC25A35 are orthologues to the yeast oxaloacetate carrier, YKL120w [29], and have 35 and 29% amino acid identity to this protein. It is therefore possible that these human solute carriers have a substrate similar to the substrate of the yeast oxaloacetate carrier.

To show the reliability of our real-time assay, we performed expressional analysis for *Slc25a8*, known as UCP2. UCP2 showed the highest expression in pituitary, which is in very good agreement with the previously published data, where mRNA for UCP2 from monkey was detected in anterior pituitary with in situ hybridization [30]. We also show that UCP2 is widely distributed in the periphery as previously described including the female reproductive system in rat that has been reported before in mouse [31].

In addition to the UCPs the ADP/ATP carriers are the second most studied members of the SLC25 family. ATP is an energy source for every living cell and a common substrate for SLC25 family proteins. The fourth isoform of the ADP/ATP carriers, named AAC4 (SLC25A31), has recently been reported [32]. There are three known isoforms of ATP-Mg transporters, named SLC25A23, 24, and 25, and here we have probably identified the fourth isoform, SLC25A41. This gene and *Slc25a23* are located on the same chromosome in human (h19), mouse (m17), and rat (r27) and they are positioned in close proximity to each other. The distances between these two genes are around 10, 6 and 3 kb in human, mouse, and rat, respectively (see Fig. 4). Considering the complex genomic structure of solute carrier genes, this distance is quite small and probably indicates the common origin and perhaps a functional pressure for their close proximity in the genome, such as a common transcriptional regulation. The predicted protein sequence of SLC25A41 grouped phylogenetically with SLC25A23 at the top of ATP-Mg carrier cluster. The SLC25A41 branched with a bootstrap value of 747, while the whole cluster branched from other SLC25 members with a highly convincing bootstrap value of 997. The predicted SLC25A41 protein shares 54–64% amino acid identity with ATP-Mg carriers. A crystal structure of the bovine ATP/ADP carrier has been described [7] and based on this model the substrate binding site for different SLC25 proteins was recently modeled, describing all possible substrate contact

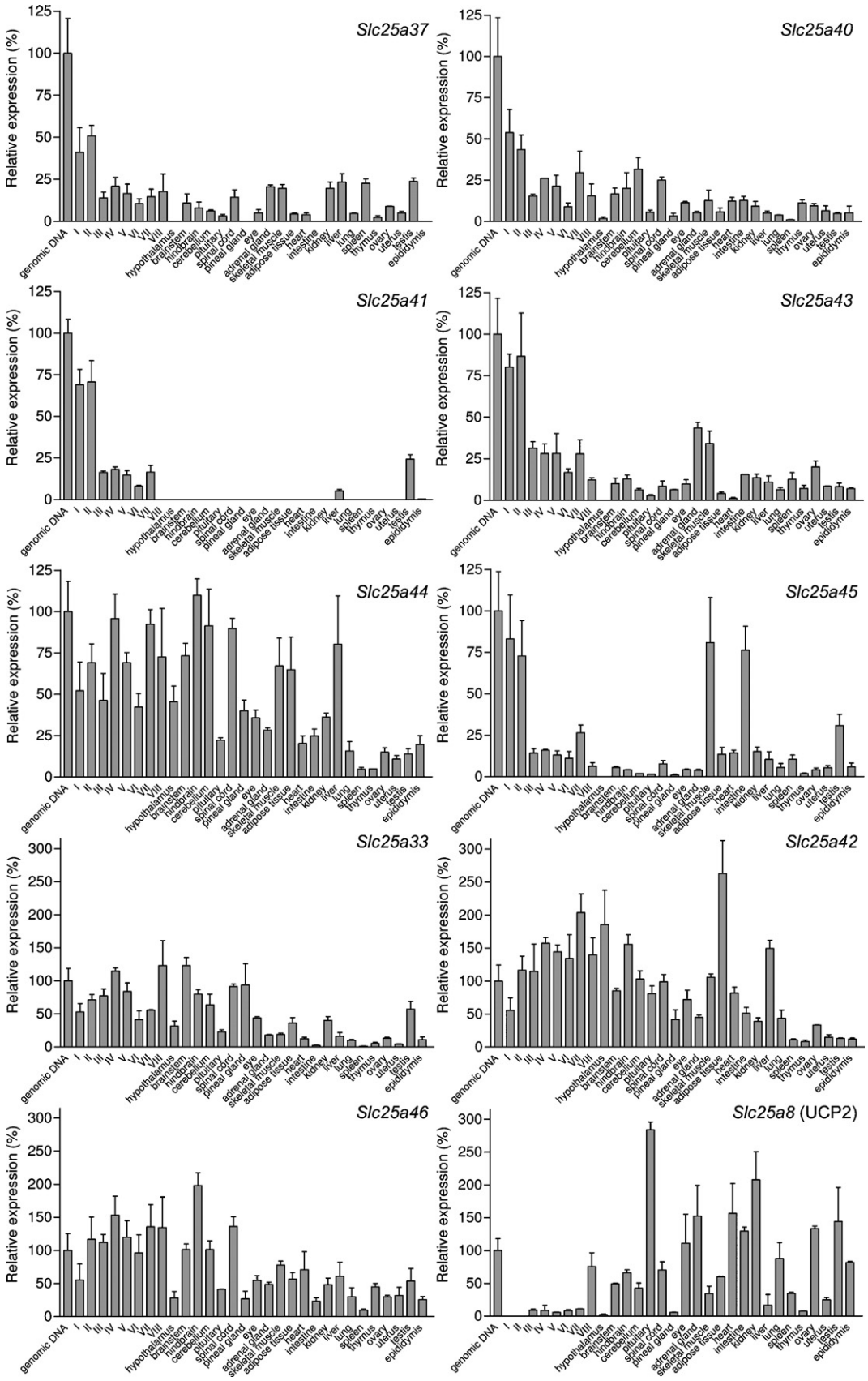

Fig. 3. Relative expression of rat mRNA for nine novel SLC25 carriers and UCP2. The coronal sections are marked with Roman numerals. Hindbrain includes cerebellum, pons, and medulla oblongata. Error bars indicate standard deviation.

Table 1
Information about novel members of SLC25 family in human, mouse, and rat

Name	Protein length (AA)	Number of exons	Chromosomal position	AA identity (%) for closest human relative with Blast search	Human relative with highest AA identity (%)
SLC25A32 (human)	295	7	Chr 8 (104481817)	SLC25A36 (30%)	SLC25A36 (30%)
Slc25a32 (mouse)	316	7	Chr 15 (38995602)		
Slc25a32 (rat)	316	7	Chr 7 (74651731)		
SLC25A33 (human)	315	7	Chr 1 (9534016)	SLC25A36 (61%)	SLC25A36 (61%)
Slc25a33 (mouse)	320	7	Chr 4 (148237103)		
Slc25a33 (rat)	320	7	Chr 5 (166836889)		
SLC25A34 (human)	338	5	Chr 1 (15808286)	SLC25A35 (45%) SLC25A11 (33%)	SLC25A35 (45%) SLC25A11 (33%)
Slc25a34 (mouse)	302	5	Chr 4 (140501676)		
Slc25a34 (rat)	302	5	Chr 5 (160520108)		
SLC25A35 (human)	315	6	Chr 17 (8133661)	SLC25A34 (45%) SLC25A11 (26%)	SLC25A34 (45%) SLC25A11, A7 (26%)
Slc25a35 (mouse)	300	5	Chr 11 (68694321)		
Slc25a35 (rat)	300	5	Chr 10 (55727781)		
SLC25A37 (human)	351	5	Chr 8 (23442460)	SLC25A28 (58%)	SLC25A28 (58%)
Slc25a37 (mouse)	338	4	Chr 14 (63778410)		
Slc25a37 (rat)	338	4	Chr 15 (49806744)		
SLC25A38 (human)	303	7	Chr 3 (39400219)	SLC25A1 (23%)	SLC25A30 (27%)
Slc25a38 (mouse)	326	7	Chr 9 (120120397)		
Slc25A38 (rat)	326	7	Chr 8 (125084567)		
SLC25A39 (human)	318	11	Chr 17 (39752897)	SLC25A40 (52%) SLC25A23 (26%)	SLC25A40 (52%) SLC25A20 (30%)
Slc25a39 (mouse)	359	11	Chr 11 (102224510)		
Slc25a39 (rat)	359	11	Chr 10 (91511138)		
SLC25A40 (human)	341	10	Chr 7 (87110217)	SLC25A39 (52%) SLC25A24 (25%)	SLC25A39 (52%) SLC25A28, A38 (26%)
Slc25a40 (mouse)	337	10	Chr 5 (8434063)		
Slc25a40 rat	337	7	Chr 4 (21497685)		
SLC25A41 (human)[a]	314	6	Chr 19 (6377402)	SLC25A23 (64%)	SLC25A23 (64%)
Slc25a41 (mouse)	312	6	Chr 17 (54722926)		
Slc25a41 (rat)	319	6	Chr 3 (11541050)		
SLC25A42 (human)	418	7	Chr 19 (19067933)	SLC25A16 (36%)	SLC25A16 (36%)
Slc25a42 (mouse)	318	7	Chr 8 (69339447)		
Slc25a42 (rat)	318	7	Chr 16 (19711606)		
SLC25A43 (human)	335	5	Chr X (118315248)	SLC25A16 (29%)	SLC25A16, A41 (29%)
Slc25a43 (mouse)	341	5	Chr X (31364298)		
Slc25a43 (rat)	329	5	Chr X (8096172)		
SLC25A44 (human)	321	3	Chr 1 (152982711)	SLC25A13 (26%)	SLC25A12 (28%)
Slc25a44 (mouse)	314	3	Chr 3 (88156573)		
Slc25a44 (rat)	314	3	Chr 2 (180514440)		
SLC25A45 (human)	304	7	Chr 11 (64900243)	SLC25A29 (25%)	SLC25A29 (25%)
Slc25a45 (mouse)	288	6	Chr 19 (5667445)		
Slc25a45 (rat)	276	5	Chr 1 (208514958)		
SLC25A46 (human)	347	8	Chr 5 (110102719)	SLC25A19 (14%)	SLC25A8 (17%)
Slc25a46 (mouse)	418	8	Chr 8 (31822955)		
Slc25a46 (rat)	418	8	Chr 18 (23991190)		

[a] Missing first exon, five amino acids.

points [33]. According to this model the yeast homologue of SLC25A23-25, Sal1p, binds ATP-Mg to the R242, K314, E318, G416, and I417, which are conserved in human ATP-Mg carriers. Interestingly, the SLC25A41 has all contact points, R40, K91, E95, G184, and I185, identical to the other ATP-Mg carriers. The expression profile of *Slc25a41* is similar to that of *SLC25A23* (APC2), which also has in general low mRNA levels [34]. The transcripts of *SLC25A23* and *SLC25A25* (APC3), but not *SLC25A24* (APC1), were previously detected in human brain tissue. The presence of *Slc25a41* mRNA in seven coronal rat brain sections, but not in brainstem, hypothalamus, or hindbrain, probably indicates a cortical expression pattern. Abundance of mRNA in CNS combined with the presence of mRNA only in two peripheral tissues might suggest a more important central function. This altogether further supports our inference that SLC25A41 might be a novel fourth isoform of ATP-Mg carrier.

The ATP-Mg cluster grouped with SLC25A16 or the so called Grave's Disease carrier (Fig. 1). SLC25A16 is thought to be responsible for transport of CoA into mitochondria [35]. Interestingly, one of the novel solute carriers, SLC25A42, shares 36% amino acid identity with SLC25A16 and they are grouped with a high bootstrap value of 961. Another novel carrier, SLC25A43, also has SLC25A16 as its closest relative

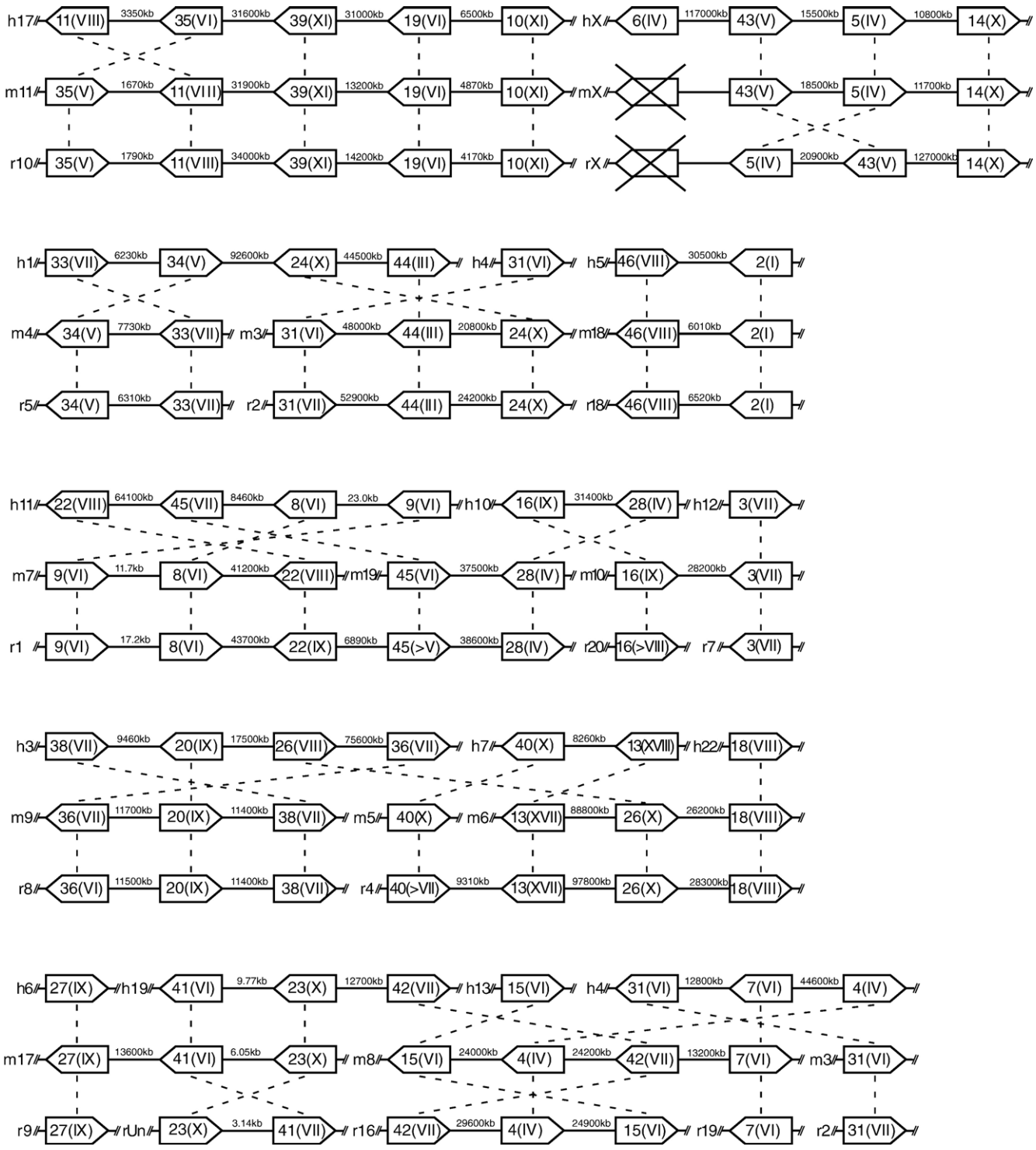

Fig. 4. Schematic presentation of chromosomal synteny for SLC25 family genes; h, human; m, mouse; r, rat. The chromosome number is next to the species. Arrowed boxes indicate the direction of the ORF. Inside each box, the Arabic numeral is the SLC25A number, while the Roman numeral denotes the number of exons.

with 29% amino acid identity. *Slc25a42* seemed to have higher expression levels than *Slc25a43*. The presence of mRNA for *Slc25a42* in all brain regions of rat, including high levels in the hypothalamus and brainstem, possibly suggests an important basal physiological function. Similarly to *SLC25A16* [36], *Slc25a42* and *Slc25a43* displayed wide peripheral distribution. Interestingly, *Slc25a42* transcript levels in male and female reproductive system, spleen, and thymus of rat were much lower than in other tested tissues. When we compared the proposed substrate binding points for SLC25A16, its yeast orthologue Leu5, and SLC25A42-43, we found small differences but surprisingly, another yeast solute carrier, YPR011c,

displayed binding points identical with those of SLC25A42, which might indicate the common substrate. We found that SLC25A42 shares 32% identity with YPR011c.

We have also identified the sequence SLC25A32, which shows 30% amino acid identity to SLC25A36 and displays orthologue relationships to three yeast solute carriers, YEL006w, YIL006w, and Flx1p. The first two, recently reported as NAD^+ transporters [37], displayed higher identity (33%) to the SLC25A32 than the third one, shown to function as a FAD transporter (30% identity) [38]. It was suggested by Palmieri [9] that there are SLC25 proteins in human with important transport functions, orthologues to those functionally characterized in yeast. Still, taking this suggestion into consideration, it is surprising how highly conserved the SLC25 proteins are in human and yeast. We compared substrate binding points and found that they are almost identical: W88/96/153, Y91/99/156, G193/192/246, V194/T193/L247, and K237/235/289 for Flx1p/SLC25A32/YIL06w, respectively. Therefore it is likely that SLC25A32 has a FAD/NAD-like substrate.

We have identified the sequence named SLC25A45, which in phylogenetic analysis, blast, and amino acid analysis showed that the closest human relative was SLC25A29 (CACL). SLC25A29 together with SLC25A20 (CACT) are known to be responsible for transport of long-chain fatty acids [9]. SLC25A29 transports palmitoylcarnitine [39], while SLC25A20 transports acylcarnitine and it has been suggested that they work cooperatively [39]. Similarly to *SLC25A29*, *Slc25a45* mRNA was detected in the brain. Like *SLC25A29* and *SLC25A20*, *Slc25a45* displayed wide peripheral distribution. Knowing that SLC25A20 and possibly SLC25A29 deficiency is life threatening [40], it would be very intriguing to investigate the function of SLC25A45.

Some of the most recently identified human solute carriers are SLC25A30 and SLC25A36. The former was identified as renal uncoupling protein [41], while the function of SLC25A36 is still unknown. Surprisingly, we identified a homologous sequence with 61% amino acid identity to SLC25A36, named SLC25A33. Once again we identified the orthologue of these two sequences in yeast, YBR192w, described as pyrimidine nucleotide transporter [42]. We detected the highest levels of *Slc25a33* in the CNS, particularly in the brainstem. The mRNA levels of *Slc25a33* in peripheral tissues were very low, suggesting that the primary function is in CNS. SLC25A44 and SLC25A46 are two other novel solute carriers with higher expression levels in CNS than in periphery. These two solute carriers and SLC25A38 are quite different from other human SLC25 family members and from each other. But according to phylogenetic analysis SLC25A38 seems to have an orthologue in yeast, YDL119c. They share 33% amino acid identity and have the same residues in the substrate binding pocket.

We have identified SLC25A37 which has highest amino acid identity to human SLC25A28 and yeast MRS3p and MRS4p. It has been shown that MRS3/4p transport iron [43]. The identity of the substrate binding amino acids implies that iron is a possible substrate for SLC25A37. We detected mRNA for *Slc25a37* in a number of tissues, including brain and peripheral organs but at low levels. The high levels of *Slc25a37* were detected in blood (data not shown). During preparation of this article, a study presenting SLC25A37, named mitoferrin, was published [44]. This study demonstrates the essential function of SLC25A37 in zebrafish and mouse as an iron transporter.

It has been previously shown that yeast solute carrier MTM1 (YGR257c) is responsible for activation of manganese-containing superoxide dismutase [45]. We have identified two proteins that possibly can perform this important function in human. We found two novel solute carriers SLC25A39 and SLC25A40, which are the orthologues of yeast MTM1. These human proteins share 52% identity with each other and 32–35% identity with MTM1. The mRNA for *Slc25a40* was widely distributed in many tissues but at low levels. We discovered that amino acid residues in the substrate binding pocket are identical in these three proteins and these are M131/125/113, A135/129/117, Y139/133/121, R232/217/205, D233/218/206, and K341/321/309 for YGR257c/SLC25A39/SLC25A40, respectively. It is therefore possible that we have identified two novel solute carriers, which could be responsible for activation of manganese-containing superoxide dismutase in human.

In summary we have identified the genes coding for 14 novel human transporters from the SLC25 family of mitochondrial carriers. We present detailed expression charts for 9 of these in rat. We provide a roadmap for the entire repertoire in human, mouse, and rat. Moreover, we identified orthologues for these proteins in yeast and show that the residues providing the contact points for the substrate are, in several cases, completely conserved in the human and yeast proteins.

Material and methods

Construction of hidden Markov models

The sequences for all known SLC25 family of proteins were downloaded from the NCBI WWW page using the Entrez data retrieval tool (http://www.ncbi.nlm.nih.gov/) based on the accession numbers obtained from the SLC database (http://www.bioparadigms.org/slc/menu.asp). This resulted in a dataset with 29 sequences with the following accession numbers: SLC25A1, gi|14165517; SLC25A2, gi|13994341; SLC25A3, gi|6031192; SLC25A4, gi|38181966; SLC25A5, gi|4502099; SLC25A6, gi|15928608; SLC25A7, gi|68532581; SLC25A8, gi|67515419; SLC25A9, gi|4507807; SLC25A10, gi|20149598; SLC25A11, gi|23844; SLC25A12, gi|21361103; SLC25A13, gi|7657581; SLC25A14, gi|4507009; SLC25A15, gi|7657585; SLC25A16, gi|27544933; SLC25A17, gi|5453918; SLC25A18, gi|47678687; SLC25A19, gi|31543632; SLC25A20, gi|54695946; SLC25A21, gi|75517681; SLC25A22, gi|23273778; SLC25A23, gi|48476342; SLC25A24, gi|33598954; SLC25A25, gi|56699401; SLC25A26, gi|31455201; SLC25A27, gi|55665525; SLC25A28, gi|28703800; SLC25A29, gi|47077783. The receptor sequences were subsequently aligned using ClustalW 1.83 [18] using default settings. From the alignments, Profile Hidden Markov Models (HMMs) were constructed using the HMMER 2.2 package [19]. The models were constructed using HMMbuild with default settings and calibrated using HMMcalibrate.

Construction of a reference database

A reference database was constructed from the RefSeq dataset version 35 (May 2005 release) (ftp://ftp.ncbi.nih.gov/ refseq/H_sapiens/) by first removing all SLC proteins that were present in the SLC database (http://www.bioparadigms.org/slc/menu.asp), in total 307 SLC proteins, from the RefSeq datafile using repeated BLASTP searches. The sequence names of all 307 SLC

proteins were then modified with a tag (_SLC_) to allow for automatic identification. The RefSeq file that was lacking all SLC sequences was then merged with the modified SLC database into a Fasta file containing 29,061 proteins. A protein database was finally constructed from this Fasta file using formatdb from the version 2.2.6 BLAST package [20].

Identification of novel members of the SLC25 family

Fasta files containing the protein versions of the human RefSeq database version 35 (May 2005 release) (ftp://ftp.ncbi.nih.gov/ refseq/H_sapiens/), the Ensembl human peptide database version 35 (April 2005 release) (ftp://ftp.ensembl.org/pub/current_homo_sapiens/data/fasta/pep/), the human Mammalian Gene Collection (MGC) cDNA database (Downloaded 6th of June 2005) (ftp://ftp1.nci.nih.gov/pub/MGC/fasta/), and the Ensembl human AbInitio protein database version 35 (April 2005 release) (ftp://ftp.ensembl.org/pub/current_homo_sapiens/data/fasta/pep/) were downloaded. The MGC database was available only as cDNA sequences and these were batch-translated into protein using a custom made JAVA program (available upon request). These protein Fasta files were searched, one database at a time in the order given above, against the HMM model using HMMsearch from the HMMER 2.2 package with a cutoff at E=10. The sequences for all hits were extracted using bash-scripts and a custom made JAVA program (available upon request) and searched against the reference database using BLASTP. The three best BLAST hits were considered and at least one of these had to be a SLC25 for that sequence to be further considered. To remove the previously known sequences all hits were aligned against the human genome using translated BLAT. The resulting PSL files were parsed, the BLAT scores were calculated according to [21] and only the highest scoring position was kept. This was done using a custom made JAVA program (available upon request). Finally, the sequences from the HMM search were aligned against the genome and all sequences that aligned to the same position in the genome as one of the previously known SLC sequences were removed using a JAVA program (available upon request). The novel hits were then merged into the set of known SLC25 proteins and the procedure was repeated for the next dataset. The order in which the datasets were used (RefSeq, Ensembl peptide, MGC, Ensembl AbInitio) ensured that the sequence most likely to be of high quality was used.

The new human sequences were searched against mouse and rat genomes using BLAT (amino acid sequence against genome) at (http://genome.ucsc.edu/). All the identified rat and mouse cDNA sequences were retrieved from the database and aligned with the human sequences.

Phylogenetic analysis

The human SLC25 sequences were combined with the sequences of 10 related transporters from yeast [22] into one Fasta file and aligned using the UNIX version of ClustalW 1.83. The default alignment parameters were applied. The sequences were then realigned and bootstrapped 1000 times using SEQBOOT from the Win32 version of the Phylip 3.6 package [23]. Protein distances were calculated using PROTDIST from Phylip 3.6. The Jones–Taylor–Thornton matrix was used for the calculation. The Neighbor-Joining trees were calculated from the 1000 different distance matrixes, previously generated with PROTDIST, using NEIGHBOR from Phylip 3.6 a3. Majority rule consensus trees were constructed with CONSENSE from the Win32 version of the Phylip 3.5 package. The trees were plotted using TreeView [24].

Animal handling and tissue isolation

Four male and two female Sprague–Dawley rats (Alab, Sweden) were kept in air-conditioned rooms (12 h dark/light cycle) at 22–23°C in an air humidity of 55%. The rats had free access to water and R36 food pellets (Labfor, Lactamin, Sweden). These conditions were maintained for 7 days, and at the end of the period the animals were sacrificed by decapitation between 3 and 6 h into the light period. Different brain regions and peripheral tissues were isolated. Two whole brains were dissected into coronal sections using a brain matrix (Pelco International, Canada) as presented in Fig. 2. The tissues were immersed into RNA-later solution (Ambion, USA), kept at room temperature for 1 h and thereafter stored at −80°C until further processed.

RNA isolation and cDNA synthesis

Individual tissue samples were homogenized by sonication in TRIzol reagent (Invitrogen, Sweden) using a Branson sonifier. Chloroform was added to the homogenate, which was then centrifuged at 10,000*g* at 4°C for 15 min. The water phase was transferred to a new tube, and RNA was precipitated with isopropanol. The pellets were washed with 75% ethanol, air dried at room temperature, and dissolved in RNase-free water. DNA contamination was removed by treatment with DNase I (Roche Diagnostics, Sweden) at 37°C for 4 h after the DNase I was inactivated by heating the samples at 75°C for 15 min. Absence of DNA contamination in the RNA was confirmed by PCR with primers for rat glyceraldehyde-3-phosphate dehydrogenase (NM_017008; tcc ctc aag att gtc agc aa, cac cac ctt ctt gat gtc atc) and RNA concentration was determined using a Nanodrop ND-1000 Spectrophotometer (NanoDrop Technologies, DE, USA). cDNA was synthesized with MMLV reverse transcriptase (GE, Sweden), using random hexamers according to the manufacturers' instructions. The quality of the cDNA was tested by PCR as described above.

Primer design and evaluation

All primers were designed with Beacon Designer v4.0 (Premier Biosoft, USA): primers for rat housekeeping genes, histone 3 (H3; NM_053985; att cgc aag ctc ccc ttt cag, tgg aag cgc agg tct gtt ttg), ribosomal protein L19 (RPL19; NM:031103; tcg cca atg cca act ctc gtc, agc ccg gga atg gac agt cac) and rat SLC genes, *Slc25a8* (UCP2) (ggc ggt ggt cgg aga tac, ggc aag gga ggt cgt ctg); *Slc25a33* (cgg gaa gaa ggcagcaag, gta ggt gga cag gac aat gg); *Slc25a37* (cag tca gcc ctc agt tgt atc, ggt gat gaa gtg gat aga ttgg); *Slc25a40* (aat gat aag ccc gtt aga attg, gga aat cca acc gtc ttc ag); *Slc25a41* (agg aat ttc ttc tac ggt gtgc, atg gga ttg atg agt gtc tgg); *Slc25a42* (cgg ctc ctc tac ttc acc tac, gaa ctg gat ggc tgc gta ag); *Slc25a43* (tct cgg ctg gct ctc ttc, tca cag tgt caa agg gaa atg); *Slc25a44* (cag agt aac aca gtc aaa tcac, ggg aga caa cat caa tggg); *Slc25a45* (gca gcc tcc atc ttg aaag, tga caa agt aca ttc cca acg); *Slc25a46* (agc cac cta gcc gag agc, tcc ttg aat atg aag acg atgc).

Quantitative real-time PCR

The cDNA was analyzed in quantitative real-time PCR with a MyiQ thermal cycler (Bio-Rad Laboratories, Sweden). Each real-time PCR with a total volume of 20 μl contained cDNA synthesized from 25 ng of total RNA, 0.25 μM each primer, 20 mM Tris/HCl (pH 8.4), 50 mM KCl, 4 mM $MgCl_2$, 0.2 mM dNTP, SYBR Green (1:50 000). Real-time PCR was performed with 0.02 u/μl *Taq* DNA polymerase (Invitrogen, Sweden) under the following conditions: initial denaturation for 3 min at 95°C, followed by 50 cycles of 15 s at 95°C, 15 s at 54–61°C (optimal annealing temperature), and 30 s at 72°C. This was followed by 84 cycles of 10 s at 55°C (increased by 0.5°C per cycle). All real-time PCR experiments were performed in duplicate and repeated twice. A negative control for each primer pair and a positive control with 25 ng of rat genomic DNA was included on each plate.

Data analysis and relative expression calculations

The MyiQ software v 1.04 (Bio-Rad Laboratories, Sweden) was used to analyze real-time PCR data and derive threshold cycle (Ct) values. Melting curves were analyzed to confirm that only one product was amplified and that it was significantly shifted compared to the melting curve for the negative control. The sample Ct values were analyzed further if the difference between those and the negative control was greater than 2; otherwise, the transcript was considered not to be expressed.

LinRegPCR [25] was used to calculate PCR efficiencies for each sample. After that Grubbs' test (GraphPad, USA) was applied to exclude outliers and calculate average PCR efficiency for each primer pair. The delta Ct method [26] was used to transform Ct values into relative quantities with standard deviations and the highest expression was normalized to 1. After that all values in each data set were divided by the relative quantity for genomic DNA. The GeNorm software [27] was used on the two housekeeping genes to calculate normalization factors for every tissue to compensate for differences in cDNA amount.

Thereafter the normalized quantities were calculated and compared to genomic DNA, which was set to 100%.

Ethical statement

All animal procedures were approved by the local ethical committee in Uppsala and followed the guidelines of European Communities Council Directive (86/609/EEC).

Acknowledgments

We thank Helgi B. Schiöth for valuable discussion during the course of the project. We thank Linnea Holmen for the preparation of the brain section figure. R.F. was supported by the Swedish Brain Foundation (Hjärnfonden). The studies were supported by Svenska Läkaresällskapet, Åke Wikberg Foundation, Lars Hiertas foundation, Thurings foundation, R.F. Kaleens foundation, the Magnus Bergwall Foundation, and Åhlens foundation.

Appendix A. Supplementary data

Supplementary data associated with this article can be found, in the online version, at doi:10.1016/j.ygeno.2006.06.016.

References

[1] J.C. Venter, et al., The sequence of the human genome, Science 291 (2001) 1304–1351.
[2] R.H. Waterston, et al., Initial sequencing and comparative analysis of the mouse genome, Nature 420 (2002) 520–562.
[3] H.B. Schioth, R. Fredriksson, The GRAFS classification system of G-protein coupled receptors in comparative perspective, Gen. Comp. Endocrinol. 142 (2005) 94–101.
[4] G. Manning, D.B. Whyte, R. Martinez, T. Hunter, S. Sudarsanam, The protein kinase complement of the human genome, Science 298 (2002) 1912–1934.
[5] F.H. Yu, W.A. Catterall, The VGL-chanome: a protein superfamily specialized for electrical signaling and ionic homeostasis, Sci. STKE. 253 (2004) re15.
[6] M.A. Hediger, et al., The ABCs of solute carriers: physiological, pathological and therapeutic implications of human membrane transport proteinsIntroduction, Pflugers Arch. 447 (2004) 465–468.
[7] E. Pebay-Peyroula, et al., Structure of mitochondrial ADP/ATP carrier in complex with carboxyatractyloside, Nature 426 (2003) 39–44.
[8] W.F. Visser, C.W. van Roermund, H.R. Waterham, R.J. Wanders, Identification of human PMP34 as a peroxisomal ATP transporter, Biochem. Biophys. Res. Commun. 299 (2002) 494–497.
[9] F. Palmieri, The mitochondrial transporter family (SLC25): physiological and pathological implications, Pflugers Arch. 447 (2004) 689–709.
[10] J.S. Kim-Han, L.L. Dugan, Mitochondrial uncoupling proteins in the central nervous system, Antioxid. Redox Signal 7 (2005) 1173–1181.
[11] W. Mao, et al., UCP4, a novel brain-specific mitochondrial protein that reduces membrane potential in mammalian cells, FEBS Lett. 443 (1999) 326–330.
[12] D. Sanchis, et al., BMCP1, a novel mitochondrial carrier with high expression in the central nervous system of humans and rodents, and respiration uncoupling activity in recombinant yeast, J. Biol. Chem. 273 (1998) 34611–34615.
[13] D. Richard, S. Clavel, Q. Huang, D. Sanchis, D. Ricquier, Uncoupling protein 2 in the brain: distribution and function, Biochem. Soc. Trans. 29 (2001) 812–817.
[14] D. Arsenijevic, et al., Disruption of the uncoupling protein-2 gene in mice reveals a role in immunity and reactive oxygen species production, Nat. Genet. 26 (2000) 435–439.
[15] Z.B. Andrews, S. Diano, T.L. Horvath, Mitochondrial uncoupling proteins in the CNS: in support of function and survival, Nat. Rev. Neurosci. 6 (2005) 829–840.
[16] J.S. Kim-Han, S.A. Reichert, K.L. Quick, L.L. Dugan, BMCP1: a mitochondrial uncoupling protein in neurons which regulates mitochondrial function and oxidant production, J. Neurochem. 79 (2001) 658–668.
[17] Z. Li, K. Okamoto, Y. Hayashi, M. Sheng, The importance of dendritic mitochondria in the morphogenesis and plasticity of spines and synapses, Cell 119 (2004) 873–887.
[18] J.D. Thompson, D.G. Higgins, T.J. Gibson, CLUSTAL W: improving the sensitivity of progressive multiple sequence alignment through sequence weighting, position-specific gap penalties and weight matrix choice, Nucleic Acids Res. 22 (1994) 4673–4680.
[19] S.R. Eddy, Profile hidden Markov models, Bioinformatics 14 (1998) 755–763.
[20] S.F. Altschul, W. Gish, W. Miller, E.W. Myers, D.J. Lipman, Basic local alignment search tool, J. Mol. Biol. 215 (1990) 403–410.
[21] W.J. Kent, BLAT–the BLAST-like alignment tool, Genome Res. 12 (2002) 656–664.
[22] L. Palmieri, M.J. Runswick, G. Fiermonte, J.E. Walker, F. Palmieri, Yeast mitochondrial carriers: bacterial expression, biochemical identification and metabolic significance, J. Bioenerg. Biomembr. 32 (2000) 67–77.
[23] J. Felsenstein, PHYLIP - Phylogeny Inference Package (Version 3.2), Cladistics 5 (1989) 164–166.
[24] R.D. Page, TreeView: An application to display phylogenetic trees on personal computers, Comput. Appl. Biosci. 12 (1996) 357–358.
[25] C. Ramakers, J.M. Ruijter, R.H. Deprez, A.F. Moorman, Assumption-free analysis of quantitative real-time polymerase chain reaction (PCR) data, Neurosci. Lett. 339 (2003) 62–66.
[26] K.J. Livak, T.D. Schmittgen, Analysis of relative gene expression data using real-time quantitative PCR and the 2(-Delta Delta C(T)) Method, Methods 25 (2001) 402–408.
[27] J. Vandesompele, et al., Accurate normalization of real-time quantitative RT-PCR data by geometric averaging of multiple internal control genes, Genome Biol. 3 (2002) (RESEARCH0034).
[28] P.J. Hoglund, D. Adzic, S.J. Scicluna, J. Lindblom, R. Fredriksson, The repertoire of solute carriers of family 6: identification of new human and rodent genes, Biochem. Biophys. Res. Commun. 336 (2005) 175–189.
[29] L. Palmieri, et al., Identification of the yeast mitochondrial transporter for oxaloacetate and sulfate, J. Biol. Chem. 274 (1999) 22184–22190.
[30] S. Diano, et al., Mitochondrial uncoupling protein 2 (UCP2) in the nonhuman primate brain and pituitary, Endocrinology 141 (2000) 4226–4238.
[31] S. Rousset, et al., Uncoupling protein 2, but not uncoupling protein 1, is expressed in the female mouse reproductive tract, J. Biol. Chem. 278 (2003) 45843–45847.
[32] V. Dolce, P. Scarcia, D. Iacopetta, F. Palmieri, A fourth ADP/ATP carrier isoform in man: identification, bacterial expression, functional characterization and tissue distribution, FEBS Lett. 579 (2005) 633–637.
[33] A.J. Robinson, E.R. Kunji, Mitochondrial carriers in the cytoplasmic state have a common substrate binding site, Proc. Natl. Acad. Sci. USA 103 (2006) 2617–2622.
[34] G. Fiermonte, et al., Identification of the mitochondrial ATP-Mg/Pi transporter. Bacterial expression, reconstitution, functional characterization, and tissue distribution, J. Biol. Chem. 279 (2004) 30722–30730.
[35] C. Prohl, et al., The yeast mitochondrial carrier Leu5p and its human homologue Graves' disease protein are required for accumulation of coenzyme A in the matrix, Mol. Cell. Biol. 21 (2001) 1089–1097.
[36] G. Fiermonte, M.J. Runswick, J.E. Walker, F. Palmieri, Sequence and pattern of expression of a bovine homologue of a human mitochondrial

transport protein associated with Grave's disease, DNA Seq. 3 (1992) 71–78.
[37] S. Todisco, G. Agrimi, A. Castegna, F. Palmieri, Identification of the mitochondrial NAD+ transporter in Saccharomyces cerevisiae, J. Biol. Chem. 281 (2006) 1524–1531.
[38] V. Bafunno, et al., Riboflavin uptake and FAD synthesis in Saccharomyces cerevisiae mitochondria: involvement of the Flx1p carrier in FAD export, J. Biol. Chem. 279 (2004) 95–102.
[39] E. Sekoguchi, et al., A novel mitochondrial carnitine-acylcarnitine translocase induced by partial hepatectomy and fasting, J. Biol. Chem. 278 (2003) 38796–38802.
[40] V. Iacobazzi, et al., Molecular and functional analysis of SLC25A20 mutations causing carnitine-acylcarnitine translocase deficiency, Hum. Mutat. 24 (2004) 312–320.
[41] A. Haguenauer, et al., A new renal mitochondrial carrier, KMCP1, is up-regulated during tubular cell regeneration and induction of antioxidant enzymes, J. Biol. Chem. 280 (2005) 22036–22043.
[42] C.M. Marobbio, M.A. Di Noia, F. Palmieri, Identification of a mitochondrial transporter for pyrimidine nucleotides in Saccharomyces cerevisiae: bacterial expression, reconstitution and functional characterization, Biochem. J. 393 (2006) 441–446.
[43] F.Y. Li, et al., Characterization of a novel human putative mitochondrial transporter homologous to the yeast mitochondrial RNA splicing proteins 3 and 4, FEBS Lett. 494 (2001) 79–84.
[44] G.C. Shaw, et al., Mitoferrin is essential for erythroid iron assimilation, Nature 440 (2006) 96–100.
[45] E. Luk, M. Carroll, M. Baker, V.C. Culotta, Manganese activation of superoxide dismutase 2 in Saccharomyces cerevisiae requires MTM1, a member of the mitochondrial carrier family, Proc. Natl. Acad. Sci. USA 100 (2003) 10353–10357.